



# OPTICAL-CAVITY-BASED PRIMARY SOUND STANDARD

Akobuije Chijioke  
Richard A. Allen  
Steven E. Fick  
David A. Long  
Benjamin J. Reschovsky  
Jared H. Strait  
Randall P. Wagner

*National Institute of Standards and Technology, Gaithersburg, MD 20899, USA  
email: akobuije.chijioke@nist.gov*

We propose an optical sound standard in which the sound pressure is directly measured by using an optical cavity to observe the induced change in the refractive index of air (acousto-optic effect). In this method, an optical cavity is coupled with an acoustic cavity, with a device to be calibrated (e.g. a microphone) inserted into one wall of the acoustic cavity. We propose that the method can achieve low-uncertainty pressure-field calibration from infrasonic (e.g. 0.1 Hz) to ultrasonic (e.g. 100 kHz) frequencies. At the lower frequencies a coupler configuration is suitable, in which the sound field is uniform in the acoustic cavity, while at higher frequencies a resonator configuration is suitable, in which a standing wave is maintained in the acoustic cavity. The method could also be incorporated into inherently traceable optical microphones. We have designed a system to demonstrate sound measurement and microphone calibration at 1 kHz using an acoustic resonator. We are constructing this system and will report on progress.

Keywords: acoustic standard, optical cavity, primary standard, refractive index

---

## 1. Introduction

The lowest-uncertainty acoustic standards at present are laboratory standard condenser microphones calibrated by the reciprocity method [1], with a calibration accuracy of about 0.04 dB (0.5 %) at acoustic frequencies around 1 kHz [2]. The reciprocity method does not realize sound pressure directly, but determines the pressure-voltage sensitivity of each of three microphones installed pairwise in a special coupler. Two of the microphones must be reciprocal, i.e., linear, passive, and capable of use as sources, noting that the magnitude of the sensitivity is the same for reciprocal devices whether used as receivers or sources. The useful frequency range (10 Hz to 20 kHz) is established by the models used to correct for the

effects of confounding phenomena. Generally, the best accuracy is achieved only by laboratory standard reciprocal microphones, although recent work [3] showed that reciprocity can be used to calibrate micro electro-mechanical microphones.

Directly measuring the sound level by optical methods can free acoustic calibration from the constraints of reciprocity, allowing primary calibration of a wide variety of devices (thus shortening the calibration chain) and also expanding the frequency range over which low uncertainty can be achieved. The development of optical sound measurement can be traced to the work of Taylor [4] in the 1970s, and has predominantly taken the form of measurements of acoustic particle velocity, achieved by seeding the air in the region of interest with small particles that scatter light. Photon correlation analysis has been developed [5] as a technique for extracting the acoustic velocity, and the method has been developed [6,7] for primary free-field acoustic calibrations. Recent work has shown high-accuracy secondary calibration using laser Doppler vibrometer measurement of diaphragm motion [8].

The variation of the refractive index of air due to sound pressure, known as the acousto-optic effect, has been exploited as a means of acoustic sensing and imaging [9–11] but low-uncertainty sound measurement has not been demonstrated. On the other hand, optical cavities are used to perform low-uncertainty measurements of refractive index [12], and also thereby of static pressure [13]. We propose that optical cavities can employ the acousto-optic effect to provide measurements of acoustic pressure, with potential accuracy sufficient to serve as primary acoustic references. In comparison to pressure and length measurement applications, an accurate measurement is required only of the change in the refractive index, not its absolute value, significantly alleviating the challenge.

A further benefit of this method of primary sound measurement is that it is traceable to quantum standards, specifically to the refractive index of helium calculated *ab initio* [14], as the refractive index of air can be measured by comparison to that of helium [15].

## 2. Measurement Concept

The optical refractive index of air varies with density, and will therefore depend on the varying pressure in an acoustic field. The dependence of the refractive index on the sound pressure is fairly independent of optical wavelength in the visible and near-infrared, and is  $2.65 \times 10^{-9} \text{ Pa}^{-1}$  at 1550 nm [16]. To accurately measure the small refractive index changes due to acoustic pressure variations, we enhance the optical phase shifts induced by the index change using a high-finesse optical cavity. By tracking the shift in the optical cavity resonance frequency we sensitively track the shift of the refractive index of the cavity medium (air). This in turn provides us with the acoustic pressure in the cavity. In order that this be useful for calibrating acoustic devices, we arrange that this pressure be the same as (or at least have a known relationship to) the sound pressure at the location of the device to be calibrated.

The phase change  $\phi$  of light of wavelength  $\lambda$  over distance  $l$  in a medium of refractive index  $n$  is

$$\phi = n l \frac{2\pi}{\lambda}. \quad (1)$$

Thus, perturbations  $\delta l$  and  $\delta n$  in the distance and index respectively cause a phase perturbation  $\delta\phi$  of

$$\delta\phi = (n \delta l + l \delta n) \frac{2\pi}{\lambda}. \quad (2)$$

The dependence of the refractive index of the medium on density thus leads to an optical phase shift induced by pressure, which can be used to measure the sound level. The change in index may vary along the optical path, and the observed index-driven optical phase change is the path-integrated value.

To increase the sensitivity  $\frac{\partial\phi}{\partial p}$  of the acoustic pressure measurement, the distance  $l$  over which the index changes and is probed by the light should be maximized,

$$\frac{\partial\phi}{\partial p} = \frac{2\pi}{\lambda} l \frac{\partial n}{\partial p}. \quad (3)$$

A convenient way to do this is to enclose the optical path through the acoustic medium between two high-reflectivity mirrors, forming a Fabry-Pérot cavity. The effective optical path length is thereby increased by a large factor (the cavity finesse  $F$ ),  $F \approx \frac{2\pi}{2-(R_1+R_2)}$ , where  $R_1$  and  $R_2$  are the power reflectivities of the mirrors. The optical phase change can conveniently be read out as the resulting change in cavity resonance frequency  $\nu_r$ .

$$\delta\nu_r = -\nu_r \left( \frac{\delta l}{l} + \frac{\delta n}{n} \right) = -\nu_r \left( \frac{\delta l}{l} + \frac{\delta\tilde{n}}{n} \right) \quad (4)$$

where  $\tilde{n}$  is the refractivity, i.e.  $n = \tilde{n} + 1$ , and the cavity resonance frequency is on the order of  $10^{14}$  Hz for visible and near-infrared light. The sensitivity of the output signal to the acoustic pressure is

$$\frac{\partial\nu_r}{\partial p} = -\nu_r \left( \frac{1}{n} \frac{\partial n}{\partial p} + \frac{1}{l} \frac{\partial l}{\partial p} \right). \quad (5)$$

For high-reflectivity mirrors, the optical resonance frequency shift for acoustic pressure amplitudes in the range of 10 Pa (114 dB) can be significantly larger than the cavity optical linewidth. An upper limit to the mirror reflectivity is set by the requirement that the optical cavity response is rapid compared to the acoustic frequency, i.e. that its linewidth is large compared to the acoustic frequency. Table 1 shows that for a finesse 10,000 optical cavity we expect a resonance frequency shift more than 30 times the cavity linewidth. We assume that we shall be comfortably able to detect a cavity resonance frequency shift of 2 % of the linewidth. This yields an expected acoustic pressure sensitivity of 0.006 Pa, corresponding to 0.06 %. As equation (5) indicates, the acoustic pressure will also cause the cavity resonance frequency to change via the effect of the pressure on the cavity length  $l$ , given the finite mechanical impedance of the mirrors and their support structure. While this can provide an alternative avenue for acoustic sensing, for primary calibration using the refractive index change it is a confounding effect.

Table 1: Parameter values and projected measurement sensitivity for an acoustic resonator type system operating at an acoustic frequency of 1 kHz and an optical wavelength of 1550 nm.

Parameter	Value
Refractive index pressure dependence, $\frac{1}{n} \frac{\partial n}{\partial p}$	$2.65 \times 10^{-9} \text{ Pa}^{-1}$
Acoustic pressure amplitude	10 Pa (114 dB)
Acoustic resonator length	0.345 m
Acoustic frequency	1 kHz
Optical wavelength	1550 nm
Cavity resonance frequency shift	5.04 MHz
Cavity finesse	10 000
Cavity length	100 mm
Cavity linewidth, $\Gamma$	150 kHz
Cavity resonance shift sensitivity	$0.02 \times \Gamma$
Acoustic pressure detection sensitivity	0.006 Pa (0.06 %, 0.005 dB)

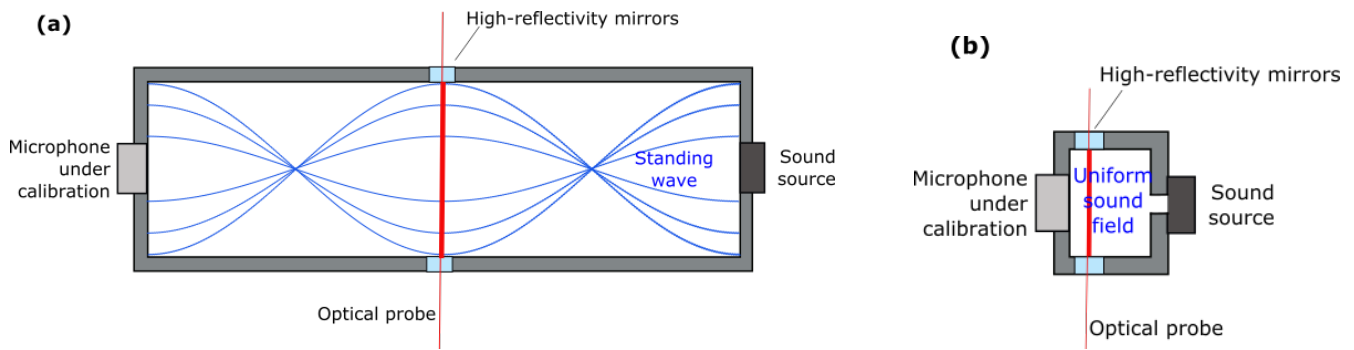


Figure 1: (a) Illustration of acoustic resonator configuration of optical sound standard. The blue curves indicate the distribution of acoustic pressure along the resonator length at different time instants; the acoustic pressure is probed at a pressure antinode of a standing plane wave. (b) Acoustic coupler configuration of optical sound standard, in which the acoustic pressure within the coupler volume is uniform.

## 2.1 Configurations

We consider a few different acoustic field configurations in which this method can be applied. The first is an acoustic plane-wave resonator, as used for particle velocity measurements [4]. This is a closed tube with a length equal to an integer number of half-wavelengths of the acoustic field at the chosen frequency of operation. When driven at such a frequency, the acoustic field in the resonator will be a standing wave. By choosing the length to be an integer number of *whole* acoustic wavelengths, the sound pressure amplitude at the midpoint will be nearly equal to that at the ends. By locating an optical cavity at the midpoint to probe the sound pressure there, we can also measure the sound pressure on a microphone diaphragm embedded flush with one end of the resonator. A resonator constructed in this manner will be suitable for calibration at a fundamental acoustic frequency equal to  $v/L$ , where  $L$  is the resonator length and  $v$  is the sound speed, and at integer multiples of this frequency. We show in Table 1 the parameters of a system designed to measure the sound pressure at 1 kHz using an acoustic resonator and an optical cavity operating at 1550 nm.

An alternative configuration is to make the dimensions of the acoustic cavity small compared to the acoustic wavelength, so that the sound pressure is nearly uniform throughout the acoustic volume. This sort of acoustic volume is called a coupler [1]. In this case the location of the optical cavity relative to the device being calibrated is relatively unimportant. A coupler of a given size will be increasingly accurate (i.e. have decreasing deviations of the sound field from uniformity) as the acoustic frequency decreases, and have an upper acoustic frequency limit of applicability.

The method can also be incorporated into a traceable optical microphone, which uses a small optical cavity (e.g. an open Fabry-Pérot cavity or a solid-state cavity that interacts with the surrounding air via an evanescent wave [19]) to track the local refractive index fluctuations. Such a device would not require calibration, being traceable via the refractive index dependence on pressure.

## 3. Readout Methods

There are several possible techniques for measuring the cavity resonant frequency and phase shift. We consider two approaches: a Pound-Drever-Hall lock and an electro-optic frequency comb.

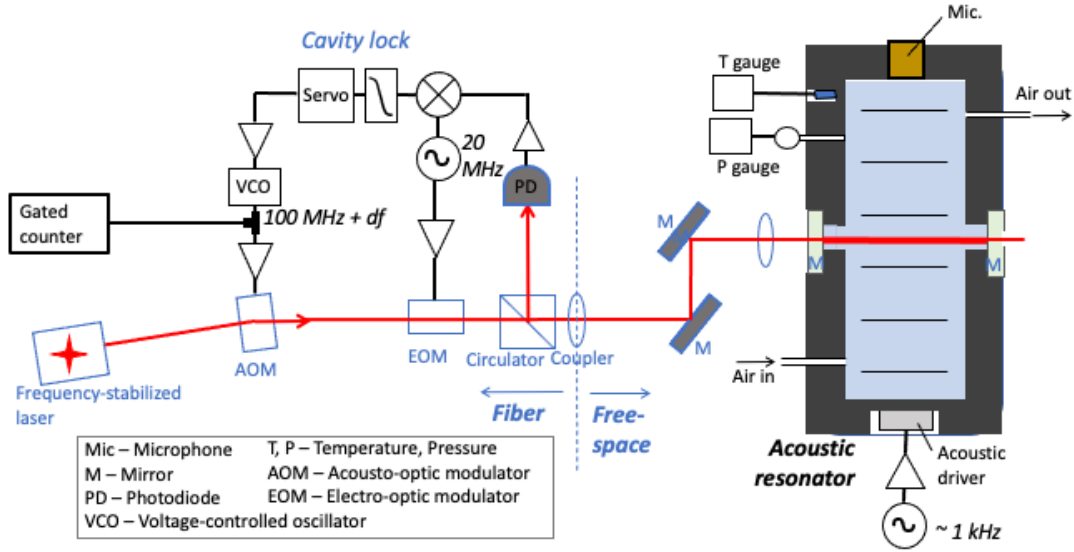


Figure 2: Pound-Drever-Hall readout system for cavity resonance frequency tracking. A gated counter with a high-repetition rate is used to make instantaneous readings of the cavity resonance frequency shift.

### 3.1 Pound-Drever-Hall lock

In the Pound-Drever-Hall (PDH) method [17, 18], the laser light is phase-modulated before it is incident on the optical cavity. The reflected light is detected by a photodiode, on which the promptly-reflected beam beats against circulating light in the cavity that has leaked back out through the input mirror. Demodulation of the photodiode output yields a first-order error signal as the laser frequency is detuned from the cavity resonance frequency. This allows the laser frequency to be servoed to the cavity resonance, oscillating with it as it varies sinusoidally due to the sound wave in the cavity.

We illustrate our implementation of PDH readout in figure 2. We use an acousto-optic modulator to apply the frequency shift to the laser light, the acousto-optic frequency offset being provided by a voltage-controlled oscillator (VCO) driven by the servo controller output. We measure the frequency of the VCO output using a frequency counter [20] with a narrow gate ( $\approx 10 \mu\text{s}$ ) and a high repetition rate ( $\approx 50 \text{ kHz}$ ). The modulation depth  $\Delta\nu_r$  of this frequency-modulated signal is the oscillation amplitude of the cavity resonance frequency, and provides us the sound pressure amplitude  $\Delta p$  according to

$$\Delta p = -\frac{\Delta\nu_r}{\nu_r} / \left( \frac{1}{n} \frac{\partial n}{\partial p} \right), \quad (6)$$

where we have assumed that change in the cavity length at the acoustic frequency is negligible.

### 3.2 Electro-optic frequency comb readout

Another approach that we are considering is readout by an electro-optic frequency comb. In this technique [21] an electro-optic phase modulator is driven with a repeating linear chirp waveform, generating a frequency comb on the output light. This light impinges on the optical cavity, and is detected in reflection. All comb teeth are fully reflected except for any that is within the cavity resonant peak width. With

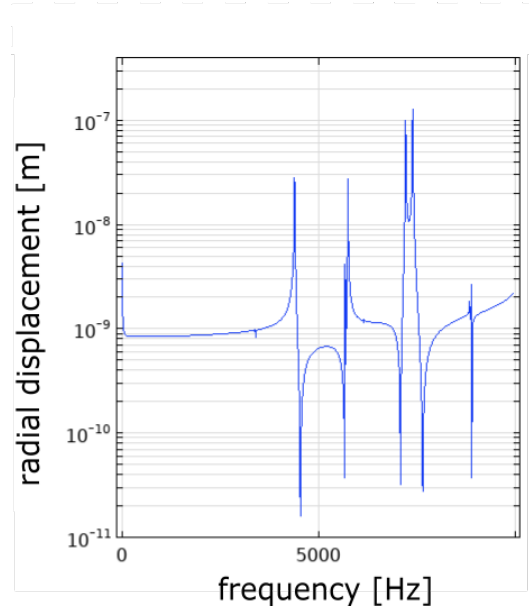


Figure 3: Frequency response of the radial position of a cavity mirror mounted on the acoustic resonator that is driven by a 1000 Pa internal pressure oscillation, from finite element simulation.

an appropriate selection of comb tooth spacing and width, the location of the the cavity resonant peak can be tracked rapidly, allowing oscillation amplitudes at frequencies in the 100s of kHz to be measured.

#### 4. Mechanical Deformation

For static elastic deformation of an infinitely long, thick cylinder of isotropic material under internal pressure, the strain  $u$  is radial and is given by [22]

$$\epsilon(r) \equiv \frac{u(r_i)}{r_i} = \frac{1 - \nu}{E} \left( \frac{r_i^2 + r_o^2}{r_o^2 - r_i^2} \right) \Delta P \quad (7)$$

where  $(\nu, E)$  are the Poisson's ratio and Young's modulus of the material,  $(r_i, r_o)$  are respectively the inner and outer radii of the cylinder, and  $\Delta P$  is the pressure difference between the inside and the outside of the cylinder. Thus, the ratio of cavity resonance shift due to geometrical length change to that due to refractive index change is given by

$$\frac{dl}{l} \bigg/ \frac{dn}{n} = \frac{u(r_i)}{r_i} \bigg/ \frac{dn}{n} = \frac{1 - \nu}{E} \left( \frac{r_i^2 + r_o^2}{r_o^2 - r_i^2} \right) \bigg/ \frac{1}{n} \frac{dn}{dP} \quad (8)$$

where we have assumed that the cavity mirror surfaces are located at the inner surface of the resonator, and that the mirror is strongly adhered to the cylinder material. For a steel cylinder with an inner diameter of 100 mm and an outer diameter of 160 mm, and 1550 nm light in air at standard atmospheric conditions, we obtain a geometrical cavity frequency shift that is  $\approx 0.3\%$  of the index cavity frequency shift.

To obtain an improved estimate of the geometrical effect, we perform a finite element simulation of the frequency response of the cylinder when driven by a pressure acting on its inner surface. We use the COMSOL [23] software package, and a geometrically accurate model of the stainless steel acoustic resonator that we have fabricated. Using a 1000 Pa acoustic pressure amplitude, we find the radial displacement amplitude at the mirror location plotted in figure 3. We see no resonant effects below  $\approx 3$  kHz, validating our rough static estimate above (at very low frequencies, we see a rigid-body recoil

effect). The optical cavity length change amplitude for a 10 Pa acoustic pressure amplitude, which taking into account the motion of both mirrors is 0.02 times the plotted value, is  $1.7 \times 10^{-11}$  m at 1 kHz. Given our cavity length of 124 mm, the geometrical cavity frequency shift is  $\frac{\Delta f}{f} = 1.38 \times 10^{-10}$ , which is 0.52 % of the index cavity frequency shift. While this was obtained with a uniform acoustic pressure distribution on the inner surface of the cylinder, subsequent simulation using a pressure field with the spatial distribution of the 1 kHz resonant mode yielded a cavity length change that agreed within a few percent. Estimating the uncertainty of the finite element simulation as 20 %, this geometrical effect introduces an uncertainty of 0.1 % to the acoustic pressure measurement. With accurate measurements of the resonator material properties we estimate that this would be reduced by a factor of  $\approx 5$ .

## 5. Discussion

A strong motivation for an optical primary standard is that it is practical for use in calibration of a wide variety of sound sources and receivers, as opposed to specially-designed reciprocal microphones. Additionally, it has the potential to achieve low uncertainty over a broader frequency range than reciprocity. The lower acoustic frequency limit will likely be set by drifts, and we estimate that electronic drifts may set a limit of  $\approx 0.01$  Hz for low-uncertainty (1 %) measurements. The upper frequency limit may be set by distortions of the sound field due to small geometrical features and imperfections; the requirement that the cavity linewidth be large compared with the acoustic frequency but small compared with the optical resonance frequency shift will also lead to an upper frequency limit. We speculate an upper acoustic frequency limit for low-uncertainty measurements in the range of  $\approx 100$  kHz. Within the core acoustic frequency range, electronic resolution of the cavity resonance frequency shift may be the largest source of uncertainty.

In comparison to photon correlation spectroscopy [6] our cavity-enhanced index-based method is less suited to free-field calibration. On the other hand, it has some important advantages: (1) The sound field measurement and the calibration are performed simultaneously, not sequentially, which is of increasing importance as the acoustic frequency decreases; (2) The acoustic pressure measurement is not dependent on knowing the acoustic impedance of the air, which is an environmentally-sensitive quantity. An optical cavity may also be advantageous for measuring particle velocity using light-scattering particles within the cavity mode volume.

In conclusion, we believe that sound standards based on measuring refractive index change using an optical cavity have the potential to realize acoustic pressure with low uncertainty from infrasonic to ultrasonic frequencies, are traceable to quantum standards, and can be developed as traceable microphones.

## REFERENCES

1. ANSI S1.15—2005/Part 2 (R2015), “Measurement Microphones— Part 2: Primary Method for Pressure Calibration of Laboratory Standard Microphones by the Reciprocity Technique”, Acoustical Society of America, New York (2005).
2. <https://www.bipm.org/kcdb/> (accessed Nov. 25, 2021).
3. R. P. Wagner and S. E. Fick, “Pressure reciprocity calibration of a MEMS microphone,” *The Journal of the Acoustical Society of America* **142**, EL251 (2017).
4. K. J. Taylor, “Absolute measurement of acoustic particle velocity,” *J. Acoust. Soc. Am.* **59**, 691–694 (1976).
5. J. P. Sharpe and C. A. Greated, “A stochastic model for photon correlation measurements in sound fields,” *J. Phys. D: Appl. Phys.* **22**, 1429 (1989)

6. T. Koukoulas, B. Piper and P. Theobald, “Gated photon correlation spectroscopy for acoustical particle velocity measurements in free-field conditions”, *J. Acoust. Soc. Am.* **133**, 156–161 (2013).
7. T. Koukoulas, L. Wu, R. Green and W.-H. Cho, “Discussion on uncertainties for potential new sound-in-air primary standard based on the optical measurement of sound pressures in free-field conditions”, *27th International Congress on Sound and Vibration*, (2021).
8. R. P. Wagner, R. A. Allen and Q. Dong, “Laser-based comparison calibration of laboratory standard microphones,” *J. Acoust. Soc. Amer. Exp. Lett.* **1**, 082803 (2021).
9. K. Nakamura, M. Hirayama and S. Ueha, “Measurements of air-borne ultrasound by detecting the modulation in optical refractive index of air” *2002 IEEE Ultrason. Symp.*, vol. 1, 609–612 (2002).
10. A. Torras-Rosell, S. Barrera-Figueroa and F. Jacobsen, “Sound field reconstruction using acousto-optic tomography,” *J. Acoust. Soc. Amer.* **13**, 3786–3793 (2012).
11. K. Ishikawa, K. Yatabe, N. Chitanont, Y. Ikeda, Y. Oikawa, T. Onuma, H. Niwa and M. Yoshii, “High-speed imaging of sound using parallel phase-shifting interferometry,” *Optics Express* **24**, 262721 (2016).
12. P. Egan and J. A. Stone, “Absolute refractometry of dry gas to  $\pm 3$  parts in  $10^9$ ,” *Applied Optics* **50**, 3076–3086 (2011).
13. P. F. Egan, J. A. Stone, J. E. Ricker and J. H. Hendricks, “Comparison measurements of low-pressure between a laser refractometer and ultrasonic manometer,” *Rev. Sci. Instrum.* **87**, 053113 (2016).
14. M. Puchalski, K. Piszczatowski, J. Komasa, B. Jeziorski and K. Szalewicz, “Theoretical determination of the polarizability dispersion and the refractive index of helium,” *Phys. Rev. A* **93**, 032515 (2016).
15. J. A. Stone and A. Stejskal, “Using helium as a standard of refractive index: correcting errors in a gas refractometer,” *Metrologia* **41**, 189–197 (2004)
16. K. P. Birch and M.J. Downs, “Correction to the updated Edlén equation for the refractive index of air,” *Metrologia* **31**, 315–316 (1994).
17. R. W. P. Drever, J. L. Hall, F. V. Kowalski, J. Hough, G. M. Ford, A. J. Munley and H. Ward, “Laser phase and frequency stabilization using an optical resonator,” *Appl. Phys. B: Photophys. Laser Chem.* **31**, 97–105 (1983).
18. R. V. Pound, “Electronic Frequency Stabilization of Microwave Oscillators,” *Rev. Sci. Instrum.* **17**, 490–505 (1946).
19. A. M Armani, R. P. Kulkarni, S. E. Fraser, R. C. Flagan and K. J. Vahala, “Label-free, single-molecule detection with optical microcavities,” *Science* **317**, 783–787 (2007).
20. Keysight model 53230A. *Certain commercial equipment, instruments, or materials are identified in this article in order to describe the experimental procedure adequately. Such identification is not intended to imply recommendation or endorsement by the National Institute of Standards and Technology, nor is it intended to imply that the materials or equipment identified are necessarily the best available for the purpose.*
21. D. Long, B. Reschovsky, F. Zhou, Y. Bao, T. LeBrun and J. Gorman, “Electro-optic frequency combs for rapid interrogation in cavity optomechanics,” *Optics Letters* **46**, 645–648 (2021).
22. W. C. Young, R. Budynas and A. M. Sadegh, *Roark’s Formulas for Stress and Strain*, McGraw-Hill Education (2012).
23. *COMSOL Multiphysics*, COMSOL Ab., Stockholm, Sweden. Version 5.6 used.